

LA-UR- 02-6463


Approved for public release;
distribution is unlimited.

Title: Combined Space and Time Convergence Analysis of a
Compressible Flow Algorithm

Author(s): James R. Kamm, CCS-2
William J. Rider, CCS-2
Jerry S. Brock, X-5

Submitted to: 16th AIAA Computational Fluid Dynamics Conference
Orlando, FL 23-26 June 2003



Los Alamos National Laboratory, an affirmative action/equal opportunity employer, is operated by the University of California for the U.S. Department of Energy under contract W-7405-ENG-36. By acceptance of this article, the publisher recognizes that the U.S. Government retains a nonexclusive, royalty-free license to publish or reproduce the published form of this contribution, or to allow others to do so, for U.S. Government purposes. Los Alamos National Laboratory requests that the publisher identify  article as work performed under the auspices of the U.S. Department of Energy. Los Alamos National Laboratory strongly supports academic freedom and a researcher's right to publish; as an institution, however, the Laboratory does not endorse the viewpoint of a publication or guarantee its technical correctness.

Form 836 (8/00)

Combined Space and Time Convergence Analysis of a Compressible Flow Algorithm

James R. Kamm, William J. Rider, Jerry S. Brock
Los Alamos National Laboratory
Los Alamos, NM 87545 USA

October 9, 2002

1 Introduction

In this study, we quantify both the spatial and temporal convergence behavior *simultaneously* for various algorithms for the two-dimensional Euler equations of gasdynamics. Such an analysis falls under the rubric of verification, which is the process of determining whether a simulation code accurately represents the code developers description of the model (e.g., equations, boundary conditions, etc.) [1]. The recognition that verification analysis is a necessary and valuable activity continues to increase among computational fluid dynamics practitioners [7]. Using computed results and a known solution, one can estimate the effective convergence rates of a specific software implementation of a given algorithm and gauge those results relative to the design properties of the algorithm. In the aerodynamics community, such analyses are typically performed to evaluate the performance of spatial integrators; analogous convergence analysis for temporal integrators can also be performed. Our approach combines these two usually separate activities into the same analysis framework.

To accomplish this task, we outline a procedure in which a known solution together with a set of computed results, obtained for a number of different spatial and temporal discretizations, are employed to determine the complete convergence properties of the combined spatio-temporal algorithm. Such an approach is of particular interest for Lax-Wendroff-type integration schemes, where the specific impact of either the spatial or temporal integrators alone cannot be easily deconvolved from computed results. Unlike the more common spatial convergence analysis, the combined spatial and temporal analysis leads to a set of nonlinear equations that must be solved numerically. The unknowns in this set of equations are various parameters, including the asymptotic convergence rates, that quantify the basic performance of the software implementation of the algorithm.

While theoretical results for convergence properties of algorithms for the Euler equations are most frequently cited for smooth problems, there are some results for flows with discontinuities [4]. In this Abstract we present preliminary results for simultaneous spatio-temporal convergence properties of two-dimensional smooth problems involving linear fields. In later work we will extend this approach to both smooth problems that involve nonlinear fields [2] as well as to problems that develop discontinuous solutions (involving, e.g., shock-waves) [5].

2 Methodology

The Euler equations summarize the conservation of mass, momentum, and energy for a compressible fluid. For a single inviscid, compressible fluid, these equations in two-dimensional Cartesian coordinates are:

$$\begin{aligned}
\frac{\partial \rho}{\partial t} + \frac{\partial(\rho u)}{\partial x} + \frac{\partial(\rho v)}{\partial y} &= 0, \\
\frac{\partial(\rho u)}{\partial t} + \frac{\partial(\rho u^2 + p)}{\partial x} + \frac{\partial(\rho u v)}{\partial y} &= 0, \\
\frac{\partial(\rho v)}{\partial t} + \frac{\partial(\rho u v)}{\partial x} + \frac{\partial(\rho v^2 + p)}{\partial y} &= 0, \\
\frac{\partial(\rho E)}{\partial t} + \frac{\partial[\rho u(E + \frac{p}{\rho})]}{\partial x} + \frac{\partial[\rho v(E + \frac{p}{\rho})]}{\partial y} &= 0,
\end{aligned} \tag{1}$$

where ρ is the mass density, (u, v) are the components of the velocity vector in Cartesian coordinates (x, y) , t is the time, $E = e + \frac{1}{2}(u^2 + v^2)$ is the specific total energy, e is the specific internal energy (SIE), and $p = p(\rho, e)$ is the pressure.

To obtain numerical solutions, these continuum equations are approximated on a grid that is discrete in both space and time. We consider an Eulerian grid onto which Eq. 1 is discretized. The corresponding solution of the discretized form of Eq. 1 is indicated as $U_{i,j}^l$, where $U = [\rho, \rho u, \rho v, \rho E]^T$ is the array of conserved variables. The quantity $U_{i,j}^l$ corresponds to $U(x_i, y_j; t_l)$, the solution at position (x_i, y_j) and time t_l . We assume a *uniform* and *equal* spatial grid with $\Delta x = \Delta y$ and *uniform* and *equal* timesteps Δt .

Modern high-resolution numerical schemes for conservation laws (see, e.g., [3, 6]) may not retain strict separation of spatial and temporal discretizations. For such methods, interaction of the spatial and temporal discretizations is at play. Such is the case for the algorithm we consider, which uses a Godunov-type method with Lax-Wendroff time differencing. In such an approach, the temporal dependence is interwoven with the spatial dependence through the self-similar solutions to local Riemann problems.

To characterize the combined spatio-temporal dependence of the error in the solution, we analyze the average per-cycle convergence properties by postulating the following error ansatz:

$$\|\xi^* - \xi_i^l\|/N_{\Delta t_l} = \mathcal{A} (\Delta x_i)^p + \mathcal{B} (\Delta t_l)^q + \mathcal{C} (\Delta x_i)^r (\Delta t_l)^s$$

$$+ o\left((\Delta x_i)^p, (\Delta t_i)^q, (\Delta x_i)^r (\Delta t_i)^s\right), \quad (2)$$

where ξ is some functional of the solution (e.g, one component of U , say, ρ), ξ^* is the corresponding exact value, ξ_i^l is the value computed on the grid of spatial zone size Δx_i with timestep Δt_i , $\|\cdot\|$ is a norm that maps its argument to a non-negative real number, $N_{\Delta t_i}$ is the number of time cycles taken to obtain the solution at the final time, A is the *spatial convergence coefficient*, p is the *spatial convergence rate*, B is the *temporal convergence coefficient*, q is the *temporal convergence rate*, C is the *spatio-temporal convergence coefficient*, and $r + s$ is the *spatio-temporal convergence rate*.

The relation in Eq. 2 averages out the position-to-position, cycle-to-cycle dependence of the computed results on Δx and Δt . In this expression, the solution norm, which is typically a discrete approximation to some integral of its argument, can be interpreted as a spatial averaging operator; that is, the norm quantifies some mean measure of the spatial behavior of its argument. The ratio of this quantity with the number of computational cycles is effectively a temporal averaging operator; unlike the spatial norm, however, this operation produces a mean per-cycle measure. Additionally, two implicit assumptions have been made in Eq. 2: (1) the zeroth-order error in the computed solution is negligible, and (2) the exact solution ξ^* can be evaluated at any grid location at the desired time.

Equation 2 contains a total of seven unknowns: A , p , B , q , C , r , and s . To solve for these quantities, we require seven independent equations. To do so, we obtain computed solutions at the same final time with the following seven combinations of spatial and temporal zoning:

$$\begin{aligned} (1) & : \{\Delta x, \Delta t\}, \\ (2) & : \{\Delta x/\sigma, \Delta t\}, \\ (3) & : \{\Delta x/\sigma^2, \Delta t\}, \\ (4) & : \{\Delta x, \Delta t/\tau\}, \\ (5) & : \{\Delta x, \Delta t/\tau^2\}, \\ (6) & : \{\Delta x/\sigma, \Delta t/\tau\}, \\ (7) & : \{\Delta x/\sigma, \Delta t/\tau^2\}, \end{aligned} \quad (3)$$

where $\sigma > 1$ is the ratio of the spatial grid sizes, and $\tau > 1$ is the ratio of the temporal grid sizes. This set of zonings is neither unique nor demonstrably optimal for obtaining solutions of Eq. 2; however, it does provide a sufficient set of independent information with which to obtain solutions for the unknowns in this equation. The set of computed solutions on these space-time grids satisfies

the following equalities at the (identical) final time:

$$\begin{aligned}
0 = f_1 &= -\|\xi^* - \xi_1\|/N_c + \mathcal{A} (\Delta x_c)^p + \mathcal{B} (\Delta t_c)^q + \mathcal{C} (\Delta x_c)^r (\Delta t_c)^s, \\
0 = f_2 &= -\|\xi^* - \xi_2\|/N_c + \mathcal{A} (\Delta x_m)^p + \mathcal{B} (\Delta t_c)^q + \mathcal{C} (\Delta x_m)^r (\Delta t_c)^s, \\
0 = f_3 &= -\|\xi^* - \xi_3\|/N_c + \mathcal{A} (\Delta x_f)^p + \mathcal{B} (\Delta t_c)^q + \mathcal{C} (\Delta x_f)^r (\Delta t_c)^s, \\
0 = f_4 &= -\|\xi^* - \xi_4\|/N_m + \mathcal{A} (\Delta x_c)^p + \mathcal{B} (\Delta t_m)^q + \mathcal{C} (\Delta x_c)^r (\Delta t_m)^s, \\
0 = f_5 &= -\|\xi^* - \xi_5\|/N_f + \mathcal{A} (\Delta x_c)^p + \mathcal{B} (\Delta t_f)^q + \mathcal{C} (\Delta x_c)^r (\Delta t_f)^s, \\
0 = f_6 &= -\|\xi^* - \xi_6\|/N_m + \mathcal{A} (\Delta x_m)^p + \mathcal{B} (\Delta t_m)^q + \mathcal{C} (\Delta x_m)^r (\Delta t_m)^s, \\
0 = f_7 &= -\|\xi^* - \xi_7\|/N_f + \mathcal{A} (\Delta x_m)^p + \mathcal{B} (\Delta t_f)^q + \mathcal{C} (\Delta x_m)^r (\Delta t_f)^s.
\end{aligned} \tag{4}$$

In these expressions, $\Delta x_c \equiv \Delta x$ is the coarse spatial grid size, $\Delta x_m \equiv \Delta x/\sigma$ is the medium spatial grid size, and $\Delta x_f \equiv \Delta x/\sigma^2$ is the fine spatial grid size; similarly, $\Delta t_c \equiv \Delta t$ is the coarse timestep, $\Delta t_m \equiv \Delta t/\tau$ is the medium timestep, and $\Delta t_f \equiv \Delta t/\tau^2$ is the fine timestep. Also, N_c , N_m , and N_f represent the number of time cycles involved in computing the solutions with the coarse, medium, and fine timesteps, respectively.

Equation 4 can be written as $\mathbf{f}(\mathbf{a}) = \mathbf{0}$, where the element of \mathbf{f} are indicated above and $\mathbf{a} \equiv [a_1, \dots, a_7]^\top \equiv [\mathcal{A}, p, \mathcal{B}, q, \mathcal{C}, r, s]^\top$. To obtain solutions to this set of nonlinear equations, we use a modified line-search based Newton's method [8]. It is straightforward to obtain closed-form expressions for the elements of the corresponding Jacobian \mathcal{J} , with elements $\mathcal{J}_{i,j} \equiv \partial f_i / \partial a_j$, the inverse of which is typically evaluated numerically in Newton's method-based routines.

To obtain solutions to Eq. 4, one must obtain the calculated solutions of Eq. 1 at the fixed final time using the spatial and temporal grids specified, and assign an initial guess for the array of unknowns that is within the domain of convergence of the iteration. The former is a matter of computer resources, whereas the latter requires some *a priori* knowledge of the algorithm of interest; the obvious choice for initial guess consists of the algorithm's theoretical convergence rate together with, say, estimates of the convergence parameter from a purely spatial convergence analysis.

3 Results

Our preliminary results for this technique are based on the evaluation of a smooth problem, i.e., one which possesses smooth initial conditions and that is allowed to evolve to a final time prior to the development of any discontinuities. The numerical solutions that we obtain with different spatial and temporal meshes are compared with the exact solution at identical final times. The convergence properties of the coded algorithm are then inferred following the procedure outlined above.

The two-dimensional, planar geometry initial conditions for this problem consist of a sinusoidal distribution of density with initially constant and uniform pressure, thermodynamically consistent specific internal energy, and uniform non-zero velocity (u_0, v_0) . The equation of state is chosen to be a polytropic

2-D Sinusoidal Density Advection Problem Initial Conditions

γ	ρ	p	e	u	v
1.4	$2 + \sin 2\pi x \sin 2\pi y$	1.0	$2.5 / (2 + \sin 2\pi x \sin 2\pi y)$	1.0	1.0

Table 1: Initial values of the adiabatic exponent γ , nondimensional density ρ , pressure p , SIE e , x -velocity u , and y -velocity v for the 2-D sinusoidal density advection problem.

gas with adiabatic exponent $\gamma = 1.4$. With periodic boundary conditions, this configuration advects the sinusoidal density and SIE distributions, which remain unperturbed, through the computational mesh. If we write the initial conditions as $f(x, y)$, then the solution at any time t is given by $f(x - u_0 t, y - v_0 t)$. The domain of interest is assigned to be the square of unit dimension centered at the origin in Cartesian geometry, i.e., $\{(x, y) : -1/2 \leq x \leq 1/2 \text{ and } -1/2 \leq y \leq 1/2\}$. The initial conditions for this problem are given in Table 1.

One caveat to this problem is that it tests only the linear fields in the governing equations. We plan to evaluate both the smooth simple wave problem proposed by Cabot [2] and the nonsmooth 1-D shock tube problems [5], both of which exercise the nonlinear fields of Eq. 1.

Calculations of all problems were carried out on uniform grids consisting of 32×32 , 64×64 , 128×128 , and 256×256 zones. Timesteps of $1/1600$, $1/3200$, $1/6400$, $1/12800$ were used. Thus, both the subsequent spatial and temporal zone sizes used in computing the convergence properties were a factor of two smaller, i.e., $\sigma = \tau = 2$ in the nomenclature of the previous section. These timesteps are well below the CFL limit for this set of calculations. It must be emphasized that the solution values must be compared at *identical locations in space at exactly the same time*. Interpolation of solutions provides values at identical spatial locations and the choice of fixed timesteps allows solutions to be obtained at the identical final time, $t = 0.1$.

Preliminary results of the suite of calculations conducted on 32×32 , 64×64 , and 128×128 grids are presented in Table 2, and results based on 64×64 , 128×128 , and 256×256 grids are given in Table 3. As shown in these tables, the spatial, temporal, and combined spatio-temporal convergence rates (i.e., p , q , and $r + s$) are each approximately two in all cases. These results are in good agreement with the design characteristics of both the spatial and temporal integrators of the code, which are all nominally second order.

4 Conclusion

In this note we have performed convergence analysis *simultaneously* in both space and time on a smooth problem for a Godunov scheme using Lax-Wendroff

$t = 0.1$ Convergence Results for 32×32 , 64×64 , and 128×128 Grids

Δt	N_c	$\mathcal{A} \times 10^2$	p	$\mathcal{B} \times 10^2$	q	$\mathcal{C} \times 10^2$	r	s
1/1600	160							
1/3200	320	1.00	1.90	0.67	1.95	1.00	0.90	0.90
1/6400	640							
1/3200	320							
1/6400	640	1.00	2.00	0.24	1.89	1.02	1.00	1.00
1/12800	1280							

Table 2: Convergence quantities for the smooth advection problem calculated with 32^2 , 64^2 , and 128^2 zones on the unit square with the indicated timesteps Δt and number of computational cycles N_c . The other parameters are defined in the text.

$t = 0.1$ Convergence Results for 64×64 , 128×128 , and 256×256 Grids

Δt	N_c	$\mathcal{A} \times 10^2$	p	$\mathcal{B} \times 10^2$	q	$\mathcal{C} \times 10^2$	r	s
1/1600	160							
1/3200	320	1.00	2.00	0.78	1.97	1.02	1.01	1.00
1/6400	640							
1/3200	320							
1/6400	640	1.00	2.00	0.28	1.89	1.05	1.01	1.00
1/12800	1280							

Table 3: Convergence quantities for the smooth advection problem calculated with 64^2 , 128^2 , and 256^2 zones on the unit square with the indicated timesteps Δt and number of computational cycles N_c . The other parameters are defined in the text.

time integration. The fundamental assumption of this analysis (Eq. 2) is that the mean per-cycle error in the computed solution varies as a polynomial in the computational cell size and computational timestep, with the exponents in this expression being the convergence rates. Unlike the direct evaluation of convergence properties for the standard spatial convergence analysis, the combined space-time analysis requires the numerical solution of a set of nonlinear verification equations. Obtaining solutions to this set of equations is more involved than directly obtaining the convergence results in the typical space-only or time-only convergence cases.

An application of this analysis is provided using a smooth advection problem. The results of our study demonstrate that the underlying advection algorithm is indeed second order in both space and time at all resolutions considered, in good agreement with the design characteristics of the numerical method. This combined spatio-temporal analysis provides concrete evidence supporting the claim of a verified implementation of the numerical algorithms.

It remains to examine this method for problems that exercise the nonlinear fields of the Euler equations. Additionally, it is of interest to examine all the roots of the system of nonlinear equations that govern the convergence properties.

Acknowledgements

This work was performed at Los Alamos National Laboratory, which is operated by the University of California for the United States Department of Energy under contract W-7405-ENG-36.

References

- [1] AIAA, *Guide for the verification and validation of computational fluid dynamics simulations*, AIAA-G-077-1998, American Institute of Aeronautics and Astronautics, Reston, VA (1998).
- [2] W. Cabot, *Simulations of a one-dimensional simple wave*, unpublished manuscript (2002).
- [3] P. Colella, E. G. Puckett, *Modern Numerical Methods for Fluid Flow*, unpublished manuscript, available at http://www.amath.unc.edu/Faculty/minion/class/C_P_Notes.pdf (1998).
- [4] B. Engquist, B. Sjögreen, The convergence rate of finite difference schemes in the presence of shocks, *SIAM J. Num. Anal.* **35**, pp. 2464–2485 (1998).

- [5] J. J. Gottlieb, C. P. T. Groth, Assessment of Riemann Solvers for Unsteady One-Dimensional Inviscid Flows of Perfect Gases, *J. Comp. Phys.* **78**, pp. 437–458 (1988).
- [6] R. J. Leveque, *Finite Volume Methods for Hyperbolic Problems*, Cambridge University Press, Cambridge, UK (2002).
- [7] W. L. Oberkampf, T. G. Trucano, Verification and Validation in Computational Fluid Dynamics, *Progress in Aerospace Sciences* **38**, pp. 209-272 (2002).
- [8] W. H. Press, B. P. Flannery, S. A. Teukolsky, W. T. Vetterling, *Numerical Recipes, The Art of Scientific Computing*, Cambridge University Press, Cambridge, UK (1992).